Bacterial Growth in the Presence of Several Resources

Ana Rita Gonçalves
Grupo de Dinâmica Não Linear – GDNL, Departamento de Física, Instituto Superior Técnico – IST, Universidade de Lisboa – UL, Avenida Rovisco Pais 1, 1049, Lisboa, Portugal
(Dated: July 2020)

There are several models describing the dynamics of a population in the presence of resources. Currently, these models are based on empirical foundations, most commonly the Monod function, and fail to include some core phenomena. We present alternatives with increasing complexity and basis on known biological processes that reproduce the observed behaviors. In addition, we analyze data collected from different experiments and also from experiments designed and executed by us, using cultures of *E. coli* to observe the bacterial growth in different conditions and find the fitting of the models. The simulations we present suggest that the Monod function may be a good approximation to some experiments but not the correct model, although further tests need to be done to validate or discard our models. We propose an experiment where the bacterial growth and nutrient concentrations are measured separately, with the intention of finding the relation between the two and calibrate them using the models here developed.

I. INTRODUCTION AND STATE OF THE ART

Living beings interact with other beings in order to feed themselves, cooperate or fight for the same resources. These interactions give rise to a highly complex network that determines the population dynamics and whether they lead to the species' coexistence or extinction. Moreover, species have the ability to adapt to changes in the environment, [2], but the connection between this phenomenon and the existing populational models is still missing. Biologists, physicists and mathematicians have been studying small ecosystems and creating models to describe the dynamics of species, [8] [14] [15]. Although they are deterministic, these models can not be implemented with basic analytical tools given their large number of variables and dependencies, which requires employing methods of dynamical systems theory.

The bacteria *E. coli*, discovered by Escherich in 1885, [5], are often chosen in experiments for their simplicity, fast growth and easy access. They are found in the intestines of warm-blooded animals, have a size of the order of 1 μm and can divide every 20 minutes, [11].

In this thesis we show the modeling of populations consuming one or multiple types of resources, reproducing and dying, using the law of mass action, [10], as well as with the Monod model, [8]. We also show the simulations resulting of these models and compare them to data obtained from our experiments and collected from other sources, [12], on *E. coli* growth curves in the presence of resources.

A. FIRST IMPORTANT GROWTH MODELS AND OBSERVATIONS

In 1798, the demographer Malthus described the first most important population growth model, [1]: when resources are unlimited, the population will grow indefinitely with a growth rate proportional to its existing number of individuals. The model can be deduced from the kinetic equation (1) assuming that the number of individuals N of a population reproduce in the presence of a resource R, at a positive rate k while the resource is not wasted in the process,

$$R + N \xrightarrow{k} R + 2N\,. \tag{1}$$

Using the law of mass action, [4][10], the time equation describing that growth can be obtained from the equation (1),

$$\begin{cases} N'(t) = k\,R(t)\,N(t) \\ R'(t) = 0 \end{cases}. \tag{2}$$

The solutions of this system of equations are

$$\begin{cases} N(t) = N(0)\,e^{k\,R\,t} \\ R(t) = R(0) \end{cases}. \tag{3}$$

In this model, resources are always available, which implies that the population explodes exponentially over time.

In 1845, the mathematician Verhulst proposed a modification to the Malthusian model, where he included the consumption of resources, [3]. Opposed to the kinetic model equation (1), the resource R is now expended as the reproduction happens,

$$R + N \xrightarrow{k} 2N. \tag{4}$$

The time equations for the population growth and resource consumption can be derived from equation (4) in the same way as before, using the mass action law, [10]:

$$\begin{cases} N' = k\,R\,N \\ R' = -k\,R\,N \end{cases} \iff \begin{cases} N' = k\,N\,(C - N) \\ R' = -k\,R\,(C - R) \end{cases} \tag{5}$$

with

$$C = R(t) + N(t) = R(0) + N(0), \tag{6}$$

that is a conservation law defining the carrying capacity constant C, that prevents the population from growing perpetually. System (5) shows that the equations are logistic, and

have the solutions

$$\begin{cases} N(t) = \dfrac{C\ e^{kCt}}{C/N(0) - 1 + e^{kCt}}, & \text{(7a)} \\ R(t) = \dfrac{CR(0)}{R(0) + [C - R(0)]e^{kCt}}. & \text{(7b)} \end{cases}$$

From the first equation in (5), we get

$$\frac{N'}{N} = k\,R\,, \tag{8}$$

a linear relation between the normalized growth rate of the population and the amount of resources.

In 1941, Monod studied a culture of *E. coli* in a medium containing glucose and proposed a sigmoidal relation between the culture's normalized growth rate and its nutrient concentration R, [8]:

$$\frac{N'}{N} = g_{max}\frac{R}{R_{1/2} + R} \tag{9}$$

where $R_{1/2}$ is the concentration for which the growth is half the maximum, g_{max}.

Although revolutionary, this empirical model described a single species in the presence of a single nutrient which is too simplistic, since species depend on different nutrients for growth and are never isolated. Moreover it could only produce accurate results for short-term evolution.

Monod also discovered the diauxic growth (Fig. 1). When bacteria are in the presence of different nutrients, they "evaluate" the energy cost of metabolizing each one *vs* the growth rate they provide, and consume them by order of most to least favorable, generating different growth rate phases over time, named diauxies. This adaptative mechanism ensures species to have the biggest growth rate when the population is small (more fragile) and provides a smaller growth rate when the population becomes bigger (smaller risk of extinction).

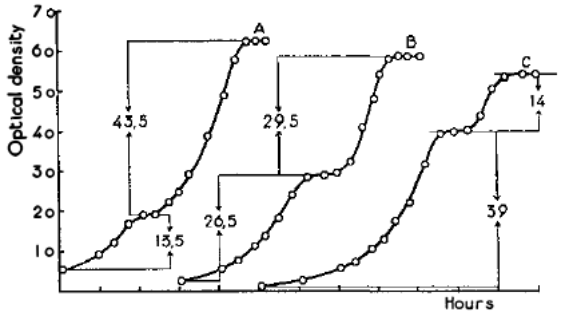

Fig. 1: *E. coli* density over time in a medium composed by glucose and sorbitol in different proportions: A: Glucose 50 µ g/ml; sorbitol 150 µ g/ml. B: Glucose 100 µ g/ml; sorbitol 100 µ g/ml. C: Glucose 150 µ g/ml; sorbitol 50 µ g/ml. Adapted from [8].

However, Monod's growth model (9) could not explain the diauxic growth he observed.

In 1969, the ecologist Robert MacArthur proposed a model describing a group of B different species (each represented by the index β) with N_β individuals, competing for J different types of common resources (each represented by the index j), and introduced different timescales for the rates of supply and consumption, [9]. MacArthur assumed the rate of growth of a population, N'_β, to be proportional to the already existing population, N_β, the number of resources of each type, R_j, their relative importance, w_j, and the probabilities of an individual of a species to consume the different nutrients, $p_{\beta j}$. The number of resources of type j varies according to their current amount, R_j, the carrying capacity associated with each resource, C_j, and to the probability of being eaten by any of the species and their population size. This model is described by the logistic equations

$$\begin{cases} N'_\beta = N_\beta M_\beta \Big(\sum\limits_j p_{\beta j} w_j R_j - R^T_\beta \Big) \\ R'_j = R_j \left[r_j \Big(1 - \dfrac{R_j}{C_j} \Big) - \sum\limits_\beta p_{\beta j} N_\beta \right] \end{cases}. \tag{10}$$

The constant R^T_β is the threshold mass of resource necessary to maintain the population, M_β is the proportion between the mass of resource and of the population it originates, and r_j is the maximum rate of resource variation. All of these constants are non negative.

In 2014, Guillaume Lambert and Edo Kussell did a series of experiments with cultures of *E. coli* feeding off glucose and lactose alternately [13]. They noticed that when consuming the same nutrient as before, the lag phases of the transitions between nutrients shortened, even if the daughter cells had never consumed the nutrients. They concluded that this phenomenon was associated with a non-genetic memory. Four years later, Cerelus et al., [16], discovered different molecular mechanisms related to this history-dependent behavior and observed that the duration of the lag phase was proportional to the amount of time the cells were feeding off the other nutrient.

B. RECENT MODELS

Based on the MacArthur's work (10), Posfai et al. presented a model in 2016, [14], that accounted for the fact that organisms work with a limited amount of energy and therefore, need to choose how to allocate different fractions in order to favor the traits that maximize the species' probability of survival. This sometimes means reducing certain performances in order to enhance others (trade-offs).

Similarly to the MacArthur' model, the population growth rates (N'_β) vary according to the current number of individuals (N_β) of each population (β), the death rates (δ_β), the nutritional values (v_j), the nutrients availability (A_j), and the consumption rates ($\alpha_{\beta j}$) of every resource j by each species β, called "metabolic strategies". The variations of resources concentrations (R'_j) are proportional to their supply rates (s_j) and decrease with the rates of consumption ($\alpha_{\beta j}$)

and degradation (d_j):

$$\begin{cases} N'_\beta = N_\beta \left[\sum_{j=1}^{J} v_j \alpha_{\beta j} A_j(R_j) - \delta_\beta \right] \\ R'_j = s_j - \sum_{\beta=1}^{B} N_\beta \alpha_{\beta j} A_j(R_j) - d_j R_j \end{cases}, \quad (11)$$

where

$$A_j(R_j) = \frac{R_j}{K_j + R_j} \quad (12)$$

is a Monod type of function with K_j being the concentration for which A_j is half the maximum. The metabolic strategies are constrained by the maximum uptake rate U_β they are capable of,

$$\sum_{j=1}^{J} w_j \alpha_{\beta j} = U_\beta. \quad (13)$$

Posfai et al. tested the possibility of coexistence of a system consisting of a group of species in the presence of three nutrients with different supply rates. In this case, by equation (13), given two metabolic strategies for a certain species, the third one is automatically determined. Thus, a triangular plot where the axes go from 0 to 1 (simplex plot), is the perfect way to visualize the distribution of metabolic strategies. Fig. 2 shows our simulations reproducing the Posfai et. al work. The results indicate that the addition of a species (in red) whose metabolic strategies allow to enclose (convex-hull) the supply rates is determinant to the future of all the other species. This, of course, discloses the importance of having certain species in an ecosystem.

In December 2018, Pacciani-Mori, Suweis and Maritan constructed a model that assumed the same equations as Posfai et al., (11), (12) and (13), but dynamic metabolic strategies instead of fixed ones, [15]. Doing so, they introduced the fact that species have the ability to adapt to changes in the nutrients' concentrations R_j. To achieve that, Pacciani-Mori et al. required species to adapt in a favorable way, i.e., so that they would evolve in order to maximize their growth rate: $\alpha'_{\beta j} \propto \partial_{\alpha_{\beta j}} \left(\sum_{j=1}^{J} v_j \alpha_{\beta j} A_j - \delta_\beta \right)$.

Now that the metabolic strategies are dynamic, there is a maximum uptake rate (U^*_β) for each species: $\sum_j w_j \alpha_{\beta j}(t) = U_\beta(t) \leq U^*_\beta$, that can be written as $Q\delta_\beta$. Therefore, the evolution of metabolic strategies (see page 4 of the supplemental material of [15]) is described by the equation

$$\alpha'_{\beta j} = \alpha_{\beta j}\, \rho\, \delta_\beta \Big[v_j A_j - \Theta\Big(\sum_{j=1}^{J} w_j \alpha_{\beta j} - Q\delta_\beta \Big) \frac{w_j}{\sum_{k=1}^{J} w_k^2 \alpha_{\beta k}} \sum_{l=1}^{J} v_l A_l w_l \alpha_{\beta l} \Big]. \quad (14)$$

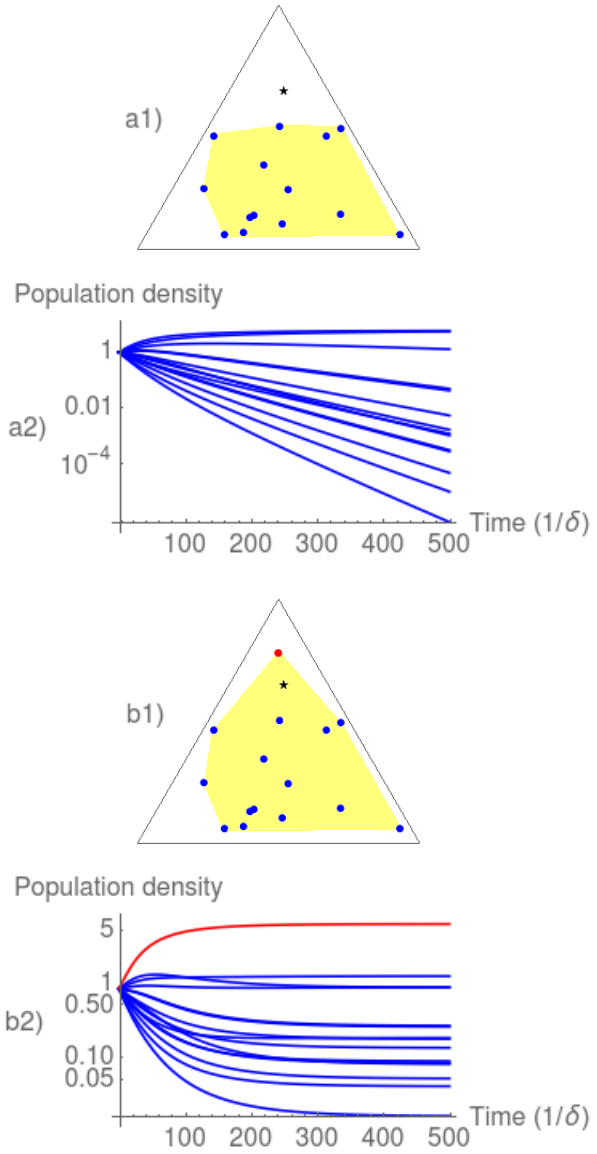

Fig. 2: a1) and b1): simplex plots with metabolic strategies of 15 species ($B = 15$) relative to 3 different resources ($J = 3$) represented by colored dots, convex-hull of metabolic strategies in yellow, and supply rates $s = (0.15, 0.19, 0.66)$ in a black star. The blue metabolic strategies were chosen randomly between 0 and 1 such that their convex-hull would not include the supply rates. The red metabolic strategies were chosen such that the new convex-hull formed by the 15 species would include the supply rates. a2) and b2): simulations obtained with model equations (11) for the evolution of the same 14 (a2) and 15 (b2) population densities, $N_\beta(t)/N_\beta(0)$, with parameters $d = 0.1$, $\delta = 0.1$, $R = 1$, $v = 1$, $K = 1$, $w = 1$, $U_\sigma = 1$ for times between 0 and $500/\delta$.

Pacciani-Mori et al. tested the model of equations (11), (12) and (13) with the addition of equation (14), for the growth of one species in the presence of two different nutrients in order to reproduce the observations of Monod. The results are shown in Fig. 3.

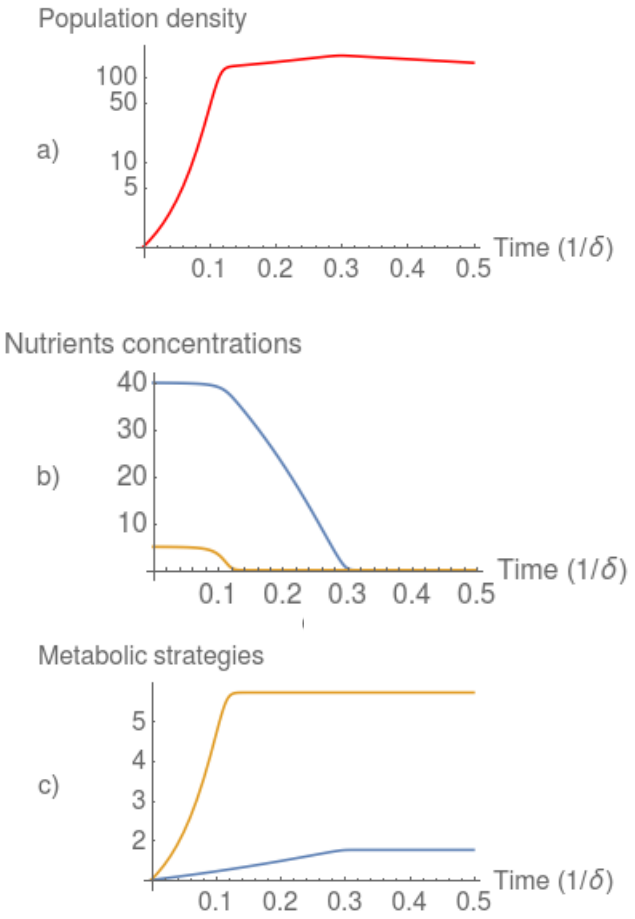

Fig. 3: Simulations obtained with model equations (11), (12), (13) and (14) for 1 population of individuals of the same species with access to 2 resources of different properties. Results of the simulation for a) the population density, b) nutrient concentrations and c) respective metabolic strategies, with parameters $\vec{v} = (2, 25)$, $\vec{w} = (1, 4)$, $\vec{K} = (1, 3)$, $Q = 25$, $\delta = 1$ and ρ for times between 0 and $500/\delta$.

The individuals consume the first resource until it ends, (Fig. 3b in orange). When this happens, the metabolic strategy corresponding to this resource changes (Fig. 3c in orange) and the population suffers a diauxic shift (Fig. 3a). Then, the individuals consume the second resource until it ends (Fig. 3b in blue). When this happens, the metabolic strategy corresponding to this resource changes (Fig. 3c in blue) and the population starts having a negative growth (Fig. 3a).

The populational models developed until now are empirical, i.e. without biological foundations. They allow us to describe the growth rate of populations in terms of parameters but they lack an explanation for what mechanisms originate variations on the rate of growth. Also, they do not take into account the necessity of more than one nutrient for growth or explain the process of cells developing the metabolic strategies. Because of this, we decided to focus on creating a model based on the known and measurable biological mechanisms of reproduction.

II. ANOTHER APPROACH TO POPULATIONAL BIOLOGY

A. MITOSIS WITH MEMORY

The first model we consider is overly simplistic, consisting in a single population of cells in the presence of an inexhaustible nutrient supply. However, in general, mitosis time, i.e., the time cells take to divide into two, depends on the pressure, temperature and availability of resources in a complex manner and for that reason we opted by a stochastic model. We assume that, initially, every cell (i) from the population divides itself after 3 hours, the first generation time (τ_{1i}). All cells are considered to have memory such that the generation time of the daughter cells (τ_{2i}) will be given by

$$\tau_{\gamma i} = \tau_{\gamma-1,\lceil \frac{i}{2} \rceil} + \epsilon \tag{15}$$

in which ϵ is a random variable obeying the normal distribution σ, i.e. $\mathcal{N}(0, \sigma^2)$.

In Fig. 5 we show the result of the simulation of a population over 40 hours obtained using the model equation (15), starting with a single cell. As a result of ϵ, the mitosis lose their initial synchronization gradually and produce a macroscopic trend curve consistent with the Malthusian model, as observed by the biologist Prescott in 1959, [17]. The distribution of the mitosis ages is Gaussian, as expected since the desynchronization comes from the the stochasticity of the variable ϵ. Rubinow [18] arrived to the same distributions using the experimental data of Prescott.

By doing a fit of the simulation the population density, N, over time for the case where $\epsilon = 0$, we discover that the curve is a power function of the form $N \approx 1.213^t$ (Fig. 4) in agreement with [10].

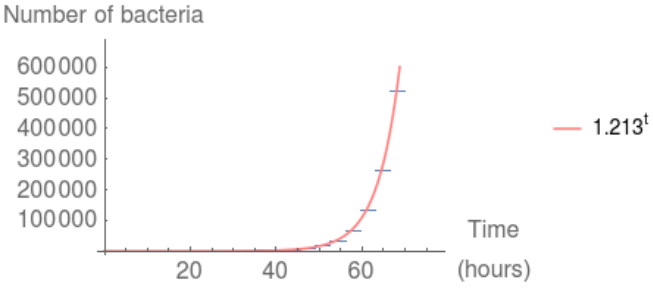

Fig. 4: Growth curve of a population for 65 hours starting with one cell and all mitosis times of 3.5 hours, and fit to a power function; the result of the fit gives $N \approx 1.213^t$ — fit executed with the `FindFit` function of the software *Mathematica* and validated by the Spearsman's rank coefficient $\rho_r = 0.999$, [7].

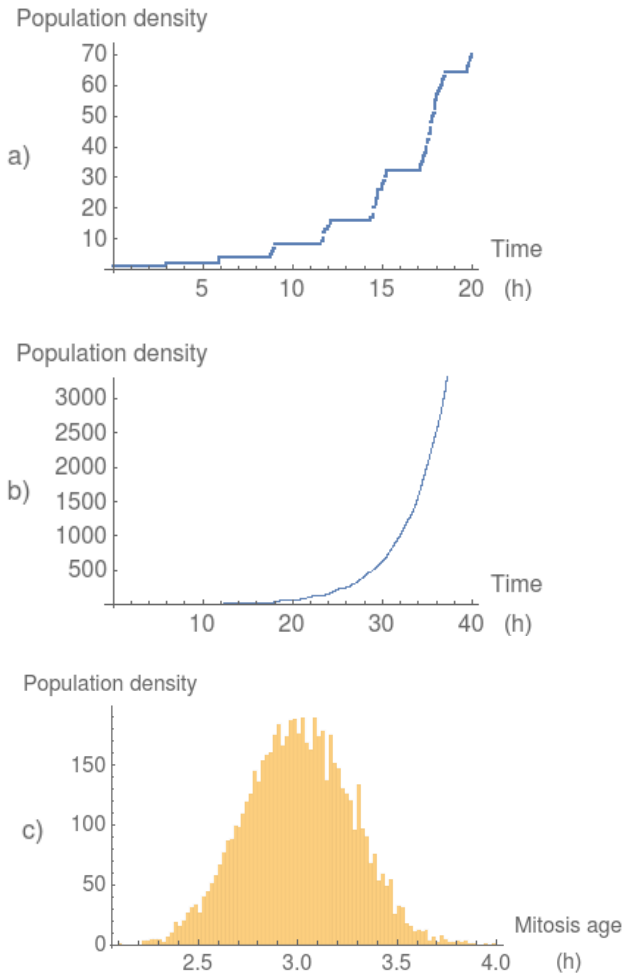

Fig. 5: a) Growth curve of a population for 20 hours starting with 1 cell with mitosis time of 3h; ϵ is randomly chosen from a normal distribution with mean value 0.0 and standard deviation 0.1; b) Growth curve of a population for 40 hours with the same conditions as in a); c) distribution of all the ages of mitosis occurred during the 40 hours population growth.

B. MITOSIS CONTROLLED BY CONSUMPTION OF A SINGLE NUTRIENT

In this model, we assume that the amount of nutrient available is limited. Cells uptake the nutrient from the medium and transform it into protein for use (metabolization). Once the cell has metabolized enough resources, P^*, it begins mitosis, [17].

Consider that the probability of a cell i finding nutrient is proportional to its quantity, $R(t)$, and the duration of the search, Δt. Also, the uptake of nutrient in reality is subject to stochastic fluctuations, for which we add the parameter λ, randomly chosen from a normal distribution $\mathcal{N}(\mu, \sigma^2)$ in each time step. Therefore, during a time interval Δt, the cell i metabolized protein $P_i(\Delta t)$ is given by $\lambda_i R(t)\Delta t$ and thus, the total amount of protein produced at an instant can be written as a recursion relation:

$$P_i(t + \Delta t) = P_i(t) + \lambda_i R(t)\Delta t. \tag{16}$$

Likewise, the amount of nutrient available at an instant is equal to the amount of nutrient there was previously minus the amount consumed by all the cells in that time interval,

$$R(t + \Delta t) = R(t) - \sum_{i=1}^{N} \lambda_i R(t)\Delta t. \tag{17}$$

We implemented the model equations (16) and (17) to simulate the growth of a population and found the sigmoidal function that best fitted the curve (Fig. 6).

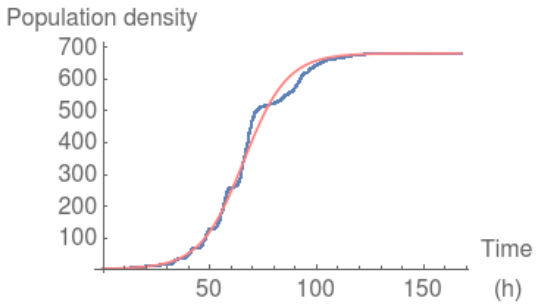

Fig. 6: In blue, simulation obtained with model equations (16) and (17) for the evolution of a population starting with 1 cell, feeding off 1 nutrient and with threshold protein $P^* = 1$ during 168 hours. The parameter λ varied according to the normal distribution with parameters $\mu = 1.5 \times 10^{-4}$ and $\sigma = 2 \times 10^{-4}$); In red, the correspondent logistic function 7a with parameters $c = 679$ and $k \approx 0.0003$ obtained with the `FindFit` function of the software *Mathematica*, corresponding to a Spearsman' rank coefficient $\rho_r = 0.927$, [7].

To study the influence of the stochasticity in the evolutions of the population and nutrient, we tested different distributions for the parameter λ. Observing Fig. 7 we can see that when the standard deviation σ increases (b to a), the desynchronization increases, i.e., the population curve becomes smoother, and macroscopically it takes a logistic shape. When the mean value μ increases (b to c), the bacteria eat in average more resources in each time step, so the population curve shifts left and becomes steeper, which translates to a faster growth that starts sooner.

Plotting the relation between the normalized growth rate and nutrient obtained from the same simulated data, we discover a linear curve, shown in Fig. 8.

From the previous analysis of the logistic and the Monod models we arrive to different relations between the normalized population growth and the amount of resource: it is linear when using the Mass action law approach, (8), and non-linear with the Monod function, (9). Thus, under our assumptions, the correct model is the logistic.

However, to test our hypothesis, and understand the relation between the Mass Action Law and the Monod model, it is necessary to perform empirical measurements and see how they relate to the corresponding growth curves obtained from these models.

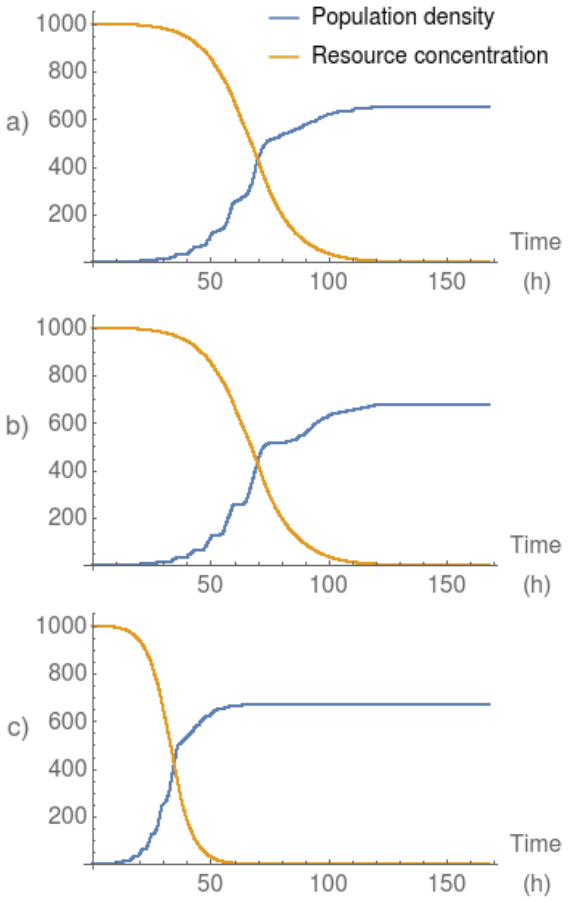

Fig. 7: Simulations obtained with model equations (16) and (17) for the evolution of a population of cells feeding off 1 nutrient during 168 hours (in blue) and for the nutrient (in orange). The parameter λ varied according to the normal distribution $\mathcal{N}(\mu, \sigma)$; a) $\mu = 1.5 \times 10^{-4}, \sigma = 10^{-3}$. b) $\mu = 1.5 \times 10^{-4}, \sigma = 2 \times 10^{-4}$; c) $\mu = 3 \times 10^{-4}, \sigma = 2 \times 10^{-4}$;

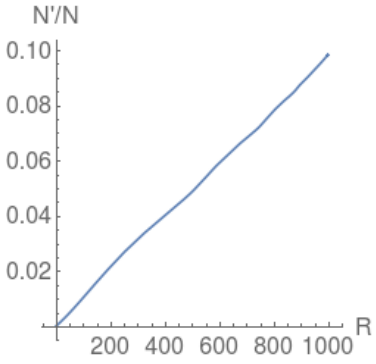

Fig. 8: N'/N vs $R(t)$ from the simulated data for the evolution of a nutrient concentration and a population of cells feeding off that nutrient for 168 hours; The parameter λ varied according to the normal distribution with $\mu = 1.5 \times 10^{-4}$ and $\sigma = 2 \times 10^{-4}$. The fit of the curve gives a linear relation $y = 10^{-4}x$ with $\chi^2 = 0.0004$.

C. FIRST EXPERIMENT AND CALIBRATION

For the calibration of the model in B, we grew a culture of *E. coli* in glucose and measured the optical densities every 20 minutes using a spectrometer. As the bacteria multiply, there is an increase in the density of the solution that contains them. Using this technique, the light that travels through the solution will be partially absorbed by it, and the emitted and transmitted intensities are measured at the wavelength of 600nm to compute a transmittance ratio. We tried to test how the empirical Monod model (9) and the logistic model obtained from first principles using mass action law approach (7a) compare with the real growth curves constructed from the data.

Procedure:
Initialy, the *E. coli* were storaged in a freezer at -80°C. We transferred a sample to a petri-dish containing solid minimal media[1] with 0.4% glycerol and took them to an incubator at 37°C to stay over night (∼12 h).

On the second day we prepared a 96-well plate with 200 µL of minimal media (MM) and 20% glycerol in 9 wells. We chose 3 colonies of the *E. coli* petri-dish and placed 3 samples of each into the previous wells. The 96-well plate was put in a temperature controlled shaker at low speed (∼ 10^2 rpm) and 37°C for the cultures to grow over night (∼12h).

On the following day, we placed the 96-well plate in a multiskan spectrometer and read the optical densities to guarantee that the biological (from the different cultures) and technical (from the same cultures) copies were all similar and in the appropriate range to start the main growth. After the reading, we transferred the cultures to separate eppendorf tubes and prepared a medium of MM with glucose in concentrations 0.400%, 0.200%, 0.100%, 0.050%, 0.025% and 0.001%. We distributed the solutions and cultures in a 96-well plate and inserted the plate in a bioscreen spectrometer for the population to grow for 36 hours while monitoring the optical densities.

Results and analysis:
Since we only have data from the optical densities, proportional to $N(t)$, and have no information of $R(t)$, we need to write equation (9) explicitly.

By Monod's idea of conversion of nutrient into biomass, [8], we have

$$N' = -kR', \tag{18}$$

from which

$$N(t) - N(0) = -k[R(t) - R(0)]. \tag{19}$$

Rearranging equation (19) and combining it with equation (9) we obtain

$$\frac{1}{N}\frac{dN}{dt} = g_{max}\frac{R(0) - [N(t) - N(0)]/k}{R_{1/2} + R(0) - [N(t) - N(0)]/k}. \tag{20}$$

[1]Minimal media is a solution containing 11.28g of M9 salts, 2mL of $MgSO_4$ 1M, 100µL of $CaCl_2$ 1M and 20mL of a 20% carbon source (0.4% final) per liter of Mili-Q (ultra pure) water; M9 is a mix of 33.9g/L Na_2HPO_4, 15g/L KH_2PO_4, 5g/L NH_4Cl and 2.5g/L NaCl.

We can write the proportionality between the optical density and the number of bacteria as

$$OD(t) = qN(t), \tag{21}$$

in which q is a positive real constant.

Substituting this relation in the model equation of (20), we obtain

$$\frac{1}{OD}\frac{d(OD)}{dt} = g_{max}\frac{R(0) - \tilde{k}[OD(t) - OD(0)]}{R_{1/2} + R(0) - \tilde{k}[OD(t) - OD(0)]}, \tag{22}$$

where $\tilde{k} = 1/(kq)$.

The same can be done with the model (7a),

$$OD(t) = \frac{m\, e^{bmt}}{\frac{m}{OD(0)} - 1 + e^{bmt}}, \tag{23}$$

in which $b = qC$ and $m = k/C$ and we see that $OD(t)$ and $N(t)$ take the same form.

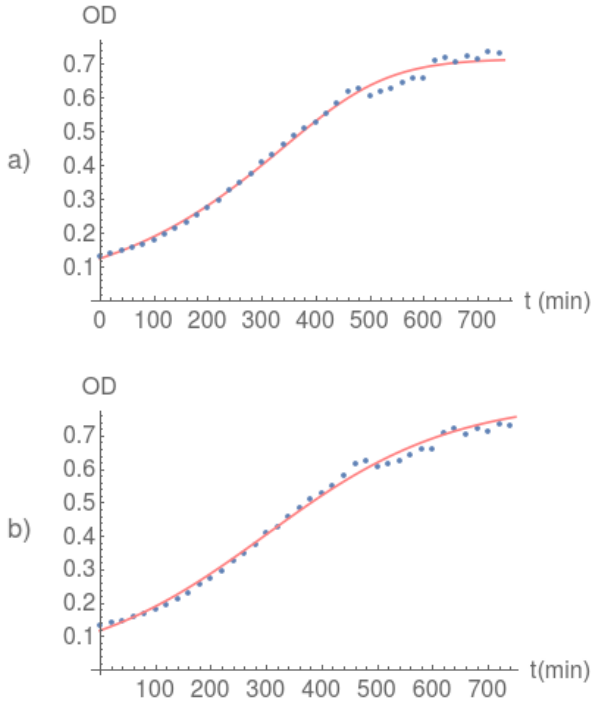

Fig. 9: Growth curve of *E. coli* population from culture 2 in minimal media with 0.400% glucose and a) fit using the Monod function. The fitted parameters for the equation (22) have results $R(0) = 0.210$, $R_{1/2} = 0.126$, $g_{max} = 0.007\,\text{min}^{-1}$, $\tilde{k} = 0.357$ and $OD(0) = 0.124$ with a $\chi^2 = 0.016$, and $\rho_r = 0.996$; b) fit using the Mass action law approach. The fitted parameters for the equation (23) have results $b = 0.007$, $m = 0.808$, $OD(0) = 0.116$, with a $\chi^2 = 0.279$, and $\rho_r = 0.996$.

Fig. 9 shows the optical densities obtained during the first 750 minutes of the growth of culture 2 in 0.400% glucose, and the comparison between the fitting of the model equations (23) and (22).

To compare the compatibility of the logistic and Monod models with the data, we tested the goodness of fit of equations (7a) and (9) using the Pearson's χ^2, [6], and the Spearman's rank correlation ρ_r coefficients, [7], tests. An example of the methods used can be found in the Appendices 4 and 5. The fits were done by first establishing the parameters visually and then by setting increasingly closer randomly generated values in order to lower the χ^2 parameter for 10^4 iterations (see appendices 4 and 5).

Although both models provide very good approximations to the data ($\chi^2 \ll 1$ and $\rho_r \approx 1$), as expected, the model with the most parameters will be easier to fit and have the smaller χ^2. Therefore, it is impossible to distinguish between the two outcomes and say which model is the valid one by this analysis.

The only way to present a solid justification for either of the models is to make independent measurements of the optical densities of the bacteria and the nutrient concentrations and do the test of Fig. 8.

D. ANALYSIS OF EXISTING DATA

In 2011 Mostovenko et al. designed an experiment consisting in a culture of *E. coli* supplied by a medium containing both glucose and lactose to study the adaptation of bacteria when consuming a different nutrients, during a diauxic growth, [12]. In Fig. 10 we have the graph from [12] containing the curves of the *E. coli* growth and the glucose consumption.

We collected the data from his work and used it to make a primary analysis of the relation between the population growth and the nutrient evolution curves. We obtained the data of the optical densities and glucose concentrations up until the 420 minutes, where the diauxie transition begins.

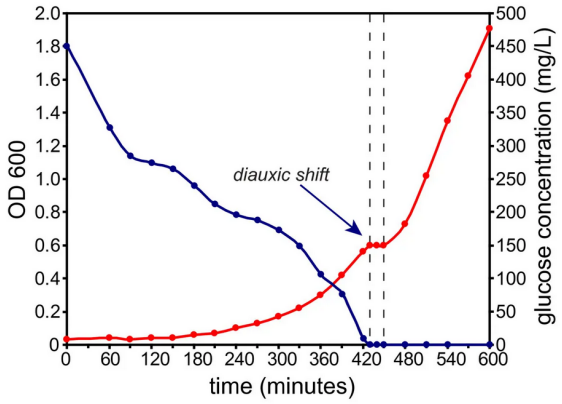

Fig. 10: Measured optical densities in red and glucose concentrations decreasing in blue. The optical density is proportional to the number of bacteria present in the media.

It is possible to identify a quasi-linear region in the initial growth of Fig. 11, until 100 mg/mL, that contrasts with the Monod model. In fact, the curve has the opposite concavity. Still, the precision of the measured optical densities and sugar concentrations does not seem sufficient to make

this analysis conclusive. Therefore, it would be necessary to elaborate an experiment where the *E. coli* grow in a single sugar medium and take measurements of the population and sugar optical densities with a great level of precision and then repeat this same study.

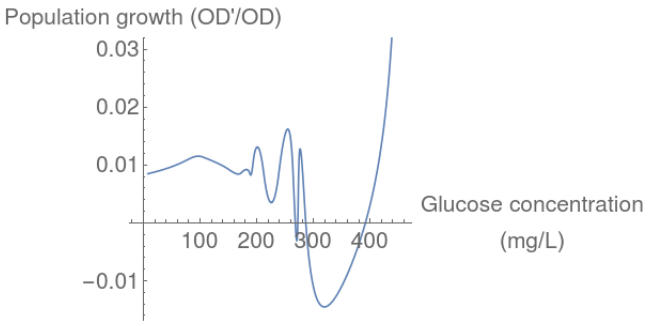

Fig. 11: Curve of the OD'/OD vs glucose concentration calculated from the first 420 minutes of data in figure 10 from the Mostovenko work [12].

E. MITOSIS CONTROLLED BY THE CONSUMPTION OF ONE NUTRIENT AND TOXICITY

In this next model, we consider that a nutrient, G, is transformed by an enzyme, E, at a constant rate k_1, creating an enzyme-carbon complex, X, (the inverse reaction also occurs, at a rate k_{-1}), that is then transformed into an absorbable energy resource R at rate k_2, and the enzyme is released — this mechanism is represented by the Michaelis-Menten kinetic diagram (24a). The resource R will then be absorbed by the N bacteria at a constant rate k_3, and the bacteria will reproduce (24b). When there is too much nutrient in the medium it becomes toxic to the *E. coli* [13], repressing growth ($\emptyset$), (24c):

$$\begin{cases} G + E \underset{k_{-1}}{\overset{k_1}{\leftrightarrows}} X \overset{k_2}{\to} E + R, & \text{(24a)} \\ R + N \overset{k_3}{\to} 2N, & \text{(24b)} \\ G + N \overset{k_4}{\to} \emptyset. & \text{(24c)} \end{cases}$$

According to the mass action law [10], the time evolution equations become

$$\begin{cases} G' = k_{-1}X - k_1GE - k_4GN \\ E' = k_{-1}X - k_1GE + k_2X \\ X' = -k_{-1}X + k_1GE - k_2X \\ R' = k_2X - k_3RN \\ N' = k_3RN - k_4GN \end{cases}, \quad (25)$$

from which we can obtain the conservation laws

$$\begin{cases} G' - E' + R' + N' = 0 \\ E' + X' = 0 \end{cases}. \quad (26)$$

As initially there are no enzyme-nutrient complexes yet formed, $X(0) = 0$. Moreover, there is no transformed nutrient in the beginning, $R(0) = 0$. Thus, the previous equations can be written as

$$\begin{cases} G - E + R + N = G(0) - E(0) + N(0) \\ E + X = E(0) \end{cases}$$

$$\Longrightarrow \begin{cases} E = [G - G(0)] + R + [N - N(0)] + E(0) \\ X = [G(0) - G] - R + [N(0) - N] \end{cases}. \quad (27)$$

Substituting the above equations (27) in (25), we obtain

$$\begin{cases} G' &= k_{-1}\Big\{ [G(0) - G] - R + [N(0) - N] \Big\} - k_4GN \\ &\quad + k_1G\Big\{ [G(0) - G] - R + [N(0) - N] - E(0) \Big\} \\ R' &= k_2 \Big\{ [G(0) - G] - R + [N(0) - N] \Big\} - k_3RN \\ N' &= k_3RN - k_4GN \end{cases}. \quad (28)$$

A steady state solution of the system of equations (28) can be solved numerically by choosing the initial conditions.

Fig. 12 shows a simulation of the growth of a population feeding off one type of nutrient and the corresponding nutrient concentration over time along with the amount of processed resource by the cells. In a) it is possible to identify a region in the beginning of the growth where the population density drops while the nutrient concentration is the highest and the resource is being processed very quickly. Based on the studies of Lambert, [13], and Cerulus, [16], this behavior is expected whenever the nutrient concentration exceeds a certain threshold. As a consequence of this initial toxicity effect, the final population density reached is lower.

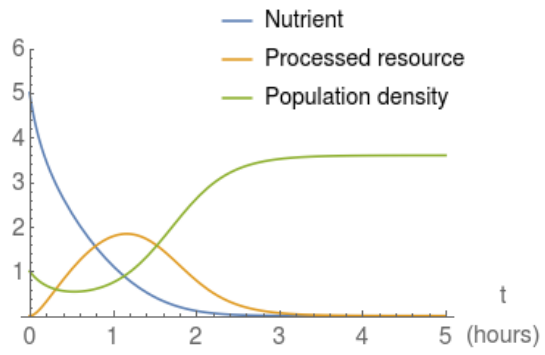

Fig. 12: Simulations obtained with the steady state model equations (28), as a function of t, for $t_{max} = 5h$, $G_0 = 5.0$, $E_0 = 2.0$, $N_0 = 1.0$, $k_{-1} = 0.1$, $k_1 = 1.0$, $k_2 = 3.0$, $k_3 = 1.0$ and $k_4 = 0.5$

F. MITOSIS CONTROLLED BY THE CONSUMPTION OF TWO NUTRIENTS AND TOXICITY

In this model we include a possible mechanism behind the occurrence of diauxies. The kinetic equation (29) describes the consumption of two different nutrients (G and S), by a population of cells (N), with the same enzymatic process as before (the enzymes E_1 and E_2 help to transform the nutrients into the corresponding complexes, X_1 and X_2 and successively into metabolizable resource R). In addition, they consider the reproduction of individuals in the presence of resource and two different toxicities associated with each nutrient.

$$\begin{cases} G + E_1 \underset{k_{-1}}{\overset{k_1}{\leftrightarrows}} X_1 \overset{k_3}{\to} E_1 + R \\ S + E_2 \underset{k_{-2}}{\overset{k_2}{\leftrightarrows}} X_2 \overset{k_4}{\to} E_2 + R \\ R + N \overset{k_5}{\to} 2N \\ G + N \overset{k_6}{\to} \emptyset \\ S + N \overset{k_7}{\to} \emptyset \end{cases} . \tag{29}$$

Repeating the steps of section E with $X_1(0) = X_2(0) = R(0) = 0$, we obtain

$$\begin{cases} G' &= k_{-1}\left[E_1(0) - E_1\right] - k_1 G E_1 - k_6 G N \\ S' &= (k_{-2} + k_2 S) X_2 - k_2 S E_2(0) - k_7 S N \\ E_1' &= (k_{-1} + k_3)\left[E_1(0) - E_1\right] - k_1 G E_1 \\ R' &= k_3\left[E_1(0) - E_1\right] + k_4 X_2 - k_5 R N \\ N' &= k_5 R N - k_6 G N - k_7 S N \end{cases} . \tag{30}$$

with

$$X_2 = G(0) - G + S(0) - S - R + N(0) - N - E_1(0) + E_1.$$

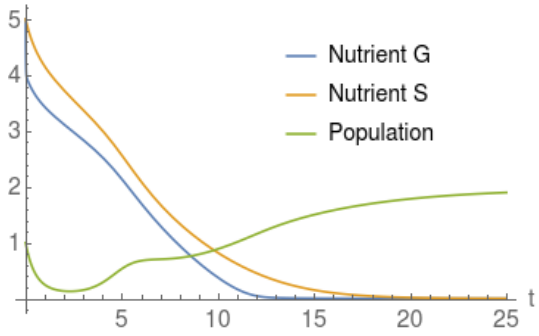

Fig. 13: Simulations obtained with the steady state model equations (30) as a function of t for $t_{max} = 25h$, $G_0 = 5$, $\alpha_0 = 5$ $E_{10} = 1$, $E_{20} = 1$, $N_0 = 1.0$, $k_{-1} = 0.1$, $k_1 = 20$, $k_{-2} = 0.01$, $k_2 = 0.1$, $k_3 = 0.2$, $k_4 = 1$, $k_5 = 2$, $k_6 = 0.2$ and $k_7 = 0.2$.

Fig. 13 shows a simulation of the growth of a population feeding off two different types of nutrient, and the corresponding nutrient concentrations over time. As in Fig. 12, it is possible to identify a region in the beginning of the growth where the population density drops while the nutrient concentrations are at the highest. After that transition, the population grows and reaches a plateau before continuing to grow. Within this setup, the diauxie appears before the extinction of the first nutrient, opposed to what Monod previously believed.

III. SECOND EXPERIMENT PROPOSAL

Bacteria take time to adapt in order to eat a sugar that they have no memory of. When bacteria eat a sugar that they already know, their starting growth happens sooner and faster. However, bacteria can transform the carbon source into another through enzymatic processes. Since we want to search for glucose-sorbitol diauxies, we should use a different sugar for the pre-culture, that is not connected through natural enzymatic processes, ex. mannose, in order to avoid favoring one of the growths.

To know the duration of the initial lag phases, the population maximum and the time necessary to reach it, it is important to first obtain the growth curves of the bacteria consuming the sugars separately, in the same setup as the experiment that will be done with both sugars.

Part 1 procedure:

Grow an *E. coli* sample in an agar plate for 24 hours in an incubator. Prepare solutions of MM with 0.2% mannose, MM with 0.1% glucose and, MM with 0.1% sorbitol. The next day, select two or more *E. coli* cultures from the agar plate and grow them in the mannose for 24 hours (pre-culture).

To know the starting number of cells after the pre-culture growth we need to relate the optical densities of some samples with the number of cultures in the same amount. By platting a small quantity of cells in an agar plate and letting them multiply in the incubator, it is possible to see scattered cultures, each originated from a single cell.

On the following day, prepare dilutions from the pre-culture on a 96-well plate to determine the optical densities and number of cells. Read the optical densities of the plate in the multiskan. Plate the dilutions in agar plates and put them in the incubator for the cultures to grow. When they are sizable enough to be seen count the number of cultures in each plate and plot them against the corresponding optical densities; the graph should be a linear tendency.

To start the culture on the single sugars, wash the cells by centrifuging, removing the supernatant and re-suspending them in MM. Grow half of the washed cells in the glucose and half in sorbitol. Repeat dilutions, optical density readings and plating to double check the starting number of cells.

Start a timer for one hour before taking them to the shaker at 37°C. Every next hour remove the tubes from the shaker, take samples of all the tubes to a 96-well plate and read the optical densities in the multiskan. Then, centrifuge another sample to take a portion of the supernatant and use Sigma-Aldrich assay kits to mix with the sugar. Read the sugar

concentrations in the multiskan. Plot the optical densities vs time as the experiment goes to see the growth curve and detect its ending.

Part 2 procedure:

For the second part of this experiment we propose to repeat the experiment above but using both sugars at the same time instead of just one and take measurements of the culture and sugars optical densities to obtain the diauxic curve and the nutrient consumption curves.

IV. CONCLUSIONS

The Monod function is an empirical model describing the relation between the growth of a population of cells and the expense of nutrient it is feeding off. Many modern models are based on the Monod's function, however none has depicted both the most essential phenomena: the diauxic growth and toxicity effects.

We presented alternative models starting with a simple construction, in section II A. There, we simulate the reproduction of cells regulated by a stochastic parameter accounting for the memory dependent behavior observed in the experiments of Lambert and Cerelus, [13] [16], yielding a Malthusian curve.

In section II B we consider that bacteria have access to a limited amount of nutrient and the mitosis is triggered by a threshold amount of protein, obtained from the metabolized nutrient, a phenomenon documented by Prescott in 1959, [17]. The simulations reproduce sigmoidal curves for the normalized population growth and nutrient concentration. The relation between the two is shown to be linear, in contradiction to the Monod's function. Moreover, it agrees with Verhulst's equation (7a), derived from the Mass Action Law, [10]. The experiment we executed (sec. II C) leaves the possibility open for the fact that a Logistic can be the correct model. In addition, the normalized growth rate and glucose concentration from Mostovenko's data, [12], exhibit a similar quasi-linear relation in the section before the diauxic shift occurs (section II D).

To take into account the toxicity phenomenon observed by Lambert, [13], and Cerelus, [16], we created a model describing a population feeding off a nutrient, in three parts: nutrient metabolization, cells reproduction and growth inhibition through direct or indirect nutrient interaction. The simulations indicate that the initial evolution of population growth observed and identified as a lag-phase can be explained by this known toxicity effect and modeled, using the law of mass action and only the basic interactions of consumption reproduction and death.

The diauxic shifts, observed when bacteria are presented to two nutrients translate into a decrease of the population growth regulated by the nutrients expense. Because of this, it is expected that the phenomenon is related to the same toxicity effect. The model of section II F was obtained by a generalization of the previous one, and the implementation of the equations suggests that the diauxic growth arises naturally without the need for an added interaction.

[1] T. R. Malthus, An Essay on the Principle of Population, 1798.

[2] C. Darwin, The Voyage of the Beagle, 1839.

[3] P. F. Verhulst, Recherches Mathematiques sur la Loi D'Accroissement de La Population, 1845

[4] P. Waage, P and C. M. Guldberg, 1864, "Studier over Affiniteten", Transactions of the Scientific Society in Christiania.

[5] T. Escherich, Die Darmbakterien des Suglings und ihre Beziehungen zur Physiologie der Verdauung, 1886.

[6] K. Pearson, 1900, "On the criterion that a given system of deviations from the probable in the case of a correlated system of variables is such that it can be reasonably supposed to have arisen from random sampling", Philosophical Magazine, Series 5.

[7] C. Spearman, 1904, The Proof and Measurement of Association between Two Things, The American Journal of Psychology.

[8] J. Monod, 1942, Recherches sur la croissance des cultures bactriennes, Hermann, Paris.

[9] R. MacArthur, 1970, Theoretical Population Biology.

[10] R. Dilão, 2006, Mathematical Models in Population Dynamics and Ecology

[11] D. Neal, Introduction to Population Biology, Cambridge Uni. Press., 2004.

[12] E. Mostovenko, A. M Deelder and M. Palmblad, Protein expression dynamics during Escherichia Coli glucose-lactose diauxie, BMC Microbiology, 2011.

[13] G. Lambert and E. Kussell, Memory and Fitness Optimization of Bacteria under Fluctuating Environments, 2014, PLOS Genetics.

[14] A. Posfai et al., 2017, Metabolic Trade-Offs Promote Diversity in a Model Ecosystem , PRL 118, 028103.

[15] L. Pacciani-Mori et al., Adaptive consumer-resource models can explain diauxic shifts and the violation of the Competitive Exclusion Principle, 2018.

[16] B. Cerulus et al., Transition between fermentation and respiration determines history-dependent behavior in fluctuating carbon sources, 2018, eLife.

[17] D. M. Prescott, Relation Between Cell Growth and Cell Division, 1959.

[18] S. I. Rubinow, Mathematical Problems in the Biological Sciences, 1973.